ARTICLE

D-Galactose Induces Necroptotic Cell Death in Neuroblastoma Cell Lines

Na Li,[1] Yangyan He,[1] Ling Wang,[1] Chunfen Mo,[1] Jie Zhang,[1] Wei Zhang,[1,2] Junhong Li,[1] Zhiyong Liao,[1] Xiaoqiang Tang,[1] and Hengyi Xiao[1]*

[1]Lab for Aging Research, State Key Laboratory of Biotherapy and Cancer Center, West China Hospital, Sichuan University, #1 Keyuan 4 Road, Gaopeng Avenue, High-tech Zone, Chengdu 610041, People's Republic of China

[2]Department of Toxicology, School of Public Health, Sichuan University, #3-17 Renminnan Road, Chengdu 610041, People's Republic of China

ABSTRACT

D-Galactose (D-gal) can induce oxidative stress in non-cancer cells and result in cell damage by disturbing glucose metabolism. However, the effect of D-gal on cancer cells is yet to be explored. In this study, we investigated the toxicity of D-gal to malignant cells specifically neuroblastoma cells. As the results, high concentrations of D-gal had significant toxicity to cancer cells, whereas the same concentrations of glucose had no; the viability loss via D-gal treatment was prominent to malignant cells (Neuro2a, SH-SY5Y, PC-3, and HepG2) comparing to non-malignant cells (NIH3T3 and LO$_2$). Differing from the apoptosis induced by H$_2$O$_2$, D-gal damaged cells showed the characters of necrotic cell death, such as trypan blue-tangible and early phase LDH leakage. Further experiments displayed that the toxic effect of D-gal can be alleviated by necroptosis inhibitor Necrostatin (Nec-1) and autophagy inhibitor 3-methyladenine (3-MA) but not by caspase inhibitor z-VAD-fmk. D-Gal treatment can transcriptionally up-regulate the genes relevant to necroptosis (Bmf, Bnip3) and autophagy (Atg5, TIGAR) but not the genes related to apoptosis (Caspase3, Bax, and p53). D-Gal did not activate Caspase-3, but prompted puncta-like GFP–LC3 distribution, an indicator for activated autophagy. The involvement of aldose reductase (AR)-mediated polyol pathway was proved because the inhibitor of AR can attenuate the toxicity of D-gal and D-gal treatment elevates the expression of AR. This study demonstrates for the first time that D-gal can induce non-apoptotic but necroptotic cell death in neuroblastoma cells and provides a new clue for developing the strategy against apoptosis-resistant cancers. J. Cell. Biochem. 112: 3834–3844, 2011. © 2011 Wiley Periodicals, Inc.

KEY WORDS: D-GALACTOSE; NEUROBLASTOMA; NECROPTOSIS; APOPTOSIS

D-Galactose (D-gal) is a kind of hexose and can be transported into cells via glucose transporters (Gluts) and then converted to glucose through enzymatic reactions [Scheepers et al., 2004]. However, D-gal can also be turned to a sugar polyol, galactitol, by aldose reductase (AR). Since galactitol could not be metabolized further, its accumulation often results in osmotic imbalance and consequentially the harmful oxidative stress in cells [Sato et al., 1996; Lu et al., 2006]. Children with genetic deficiency of the enzymes that are necessary for transforming galactose to glucose often suffer from hypergalactomia with some neural and hepatic abnormalities [Kowluru et al., 1997]. Experimentally, loading 8–16 g/L of D-gal to cultured MEF cells induced senescent phenomena [Cui et al., 1997], and the animals accepting D-gal administration often carried signs of oxidative stress in blood and various tissues [Lei et al., 2008; Zhong et al., 2009]. However, to our knowledge, no report has taken the cytotoxic effect of D-gal on tumor cells as study focus.

Cell toxicity has been utilized to develop anti-tumor drugs. Many anti-tumor drugs act as inducers of cell death by promoting apoptosis procedure [Bold et al., 1997]. However, apoptosis-inducing drugs do not work efficiently on drug-resistant cancer because many of these cancers carry either mutated p53 gene, the encoding protein of which is important for growth inhibition and apoptosis of cells, or other obstacles on apoptotic pathway [Tweddlea et al., 2003]. Recently, the efforts has been emerging to identify new anti-cancer drugs that would induce non-apoptotic cell death [Choi, 2005]. At least two research groups claimed that they had found cell death inducers that can act via necroptosis- and

autophagy-related pathway and work in an apoptosis-independent manner [Hu and Xuan, 2008; Pan et al., 2010].

Necroptosis and autophagy are two recently identified programmed cell death processes. Necroptotic cell death is p53- and caspase-independent but RIP1-dependent [Cho et al., 2009]. Different from apoptotic cell death, necroptosis does not result in condensed chromatins, shrank cell body or regular fragmented genome, but featured by damaged integrity of cytoplasm membrane, which can be confirmed by LDH leakage and trypan blue staining [Degterev et al., 2008]. At the molecular level, necroptotic cells usually have higher expression of the genes that symbolize the RIP-cascades, such as Bmf and Bnip3 [Hitomi et al., 2008; Kim and Milner, 2011], but do not elevate the expression or activation of the genes that link to apoptosis, such as p53, Bax and caspases-3. Autophagy is a process involving lysosomal protein degradation and over-activated autophagy has been linked to necroptotic cell death [Kroemer et al., 2009; Bonapace et al., 2010]. Increased distribution of microtubule associated protein light chain 3 (LC3) in lysosome membrane has been used as a marker of activated autophagy [Kabeya et al., 2000], and Atg-family proteins and TIGAR are known functionally necessary for autophagy [Pua et al., 2007].

Given the importance of cancer therapy and the existing knowing about the harmful influence of D-gal to cells and tissues, we planned this study to investigate the cytotoxic effect of D-gal on cancer cells. The study is specifically focused on: (1) Setting up an in vitro system where D-gal can induce the death of cancer cells. We chose neuronal malignant cell lines due to the neural sensitivity of D-gal [Zhang et al., 2004; Cui et al., 2006]; (2) Comparing in parallel the effects of D-gal and glucose to identify the unique characters of D-gal; (3) Characterizing the cell death that induced by D-gal based on known features of different mechanisms of cell death; (4) Verifying the involvement of polyol pathway in D-gal induced cell death. We believe this study could provide informative data in the study for tumor therapy, especially the therapy of neuroblastoma.

MATERIALS AND METHODS

REAGENTS

Cell lines were purchased from American Type Culture Collection (Manassas, USA). Dulbecco's modified Eagle medium (DMEM) and 1640 medium were purchased from Gibco BRL (Grand Island, NY). Fetal bovine serum (FBS) was purchased from Fumeng (Shanghai, China), L-glutamine, 3-(4,5-dimethyl-2-thiazolyl)-2,5-diphenyl-2H-tetrazolium bromide (MTT), D-galactose, Glucose, Necrostatin-1(Nec-1) and 3-Methyladenine (3-MA) were obtained from Sigma (St. Louis, MO). z-VAD-fmk and propidium iodide (PI) were purchased from KeyGen (Shanghai, China). Sorbinil was from Dr. Bhatnagar's lab [Bhatnagar et al., 2001], Trizol reagent was purchased from Invitrogen (Carlsbad, CA), the reagents used for real time RT-PCR were from TaKaRa (Dalian, China). The kits for the quantification of malondialdehyde (MDA) and lactate dehydrogenase (LDH) activity were purchased from Jiancheng (Nanjing, China). pEGFP–LC3 construct has been described previously [Kabeya et al., 2000].

CELL CULTURE AND VIABILITY ASSAY

Mouse neuroblastoma cell line Neuro2a (N2a), human neuroblastoma cell line SH-SY5Y, human prostate cancer cell line PC-3 and mouse fibroblast cell line NIH3T3 were cultured in DMEM supplemented with 10% FBS, 100 U/ml penicillin, and 100 μg/ml streptomycin. Human hepatoma cell line HepG2 and human hepatocyte cell line LO$_2$ were cultured in RPMI 1640 with 10% FBS. Cells were maintained at 37°C with 5% CO$_2$, and treated with D-gal or glucose in the concentrations and the time periods as indicated in figure legends. Morphological assessments were conducted under microscope. Cell viability was evaluated by MTT assay as described by Ghelli et al. [2003]. Three independent experiments were performed.

FLOW CYTOMETRY ANALYSIS

N2a cells were prepared and treated as described in the legend of Figure 2C, and then cell cycle distribution was analyzed by flow-cytometry after staining by PI, according to the manufacturer's instruction. The obtained results analyzed by the Cell Quest software. Three separate experiments were performed.

COLONY FORMATION ASSAY

Colony formation assay was performed as previously described [Lee et al., 2009]. Briefly, N2a cells were seeded in six-well plates at 1×10^3 cells per well, followed by nil treatment and the treatment of either D-gal or glucose at 40 g/L for 24 h. Then the medium was changed to blank complete medium in all wells. After 11 more days, cell colonies were stained with Giemsa. Colonies containing more than 50 cells were qualified to be scored, and counted from three wells in each treatment group. Colony formation efficiency of D-gal- or glucose-treated group against untreated group was shown as CFE. Three separate experiments were performed.

CELL ATTACHMENT ASSAY

The assay was performed as H.S. Marr's method [Marr and Edgell, 2003] with minor modification. Briefly, N2a cells were treated with either D-gal or glucose at 40 g/L for 24 h. These cells were trypsinized, reseeded at 5×10^5 cells per well in six-well plate. After 30 min incubation, cells in 5 equivalent pre-specified fields per well were counted, then the unattached cells were removed followed by gently washing with PBS. The remaining attached cells in the same fields were counted. The counts from three wells of the same treatment were aggregated and used for statistic analysis. Three separate experiments were performed.

CELL DEATH ANALYSIS

N2a and SH-SY5Y cells were plated into 96-well or 24-well plates and cultured in complete medium overnight. After treated with D-gal at different concentrations for 24 h, both adherent and floating cells in duplicated wells were stained by trypan blue and counted under phase contrast microscope. The rate of trypan blue-positive cells against total cells was calculated from 5 visual fields under each treatment. Similarly, the cells were stained by DAPI according to the manufacturer's instruction and observed under inverted fluorescence microscope (Nikon, TE2000). The rate of condensed

nucleolus against total cells was calculated in 5 visual fields from each treatment. Three separate experiments were performed.

In separate experiments, Lactate dehydrogenase (LDH) released into culture medium was measured after incubation with or without D-gal for indicated periods of time. LDH activity assay was conducted based on the method published earlier [Krady et al., 2005].

CHEMICAL INHIBITOR UTILIZATION

For pathway inhibition, N2a cells were seeded 1 day earlier before experiments. The chemical inhibitors were incorporated in the medium for the optimized time periods: 1 h for z-VAD-fmk (10 μM), 3 h for Nec-1(10 μM) and 3-MA (2 mM), and 24 h for Sorbinil (10 μM), followed by D-gal treatment for 24 h or H_2O_2 treatment for 2 h. The effects of these inhibitors on the role of D-gal and H_2O_2 in inducing cell death were detected by cell viability assay.

WESTERN BLOTTING

N2a cells were lysed with Laemmli Sample Buffer followed by heat denaturation. Fifty micrograms of whole cell proteins were applied to 12% SDS–polyacrylamide gel. After electrophoresis, the proteins were transferred to PVDF membranes, which were blocked in the buffer containing 5% nonfat dry milk. The membranes were probed with β-actin and cleaved caspase-3 antibodies (Santa Cruz) at 4°C overnight, and then washed and incubated with HRP-conjugated secondary antibody and finally visualized using Chemiluminescent ECL reagent (Millipore, MA, USA).

GFP–LC3 DISTRIBUTION ASSAY

The cellular distribution of transfected GFP-tagged LC3 protein (GFP–LC3) in N2a cells was investigated according to the protocol as described [Xiong et al., 2010]. Briefly, N2a cells were seeded in 24-well plate and then transfected with the expression plasmid of GFP–LC3 (pGFP–LC3) capsuled by lipofectamin2000 (Invitrogen, Inc.). After 24 h, 60 g/L D-gal was added for additional 24 h of culture. The distribution of GFP–LC3 in cells was examined under fluorescence microscope. For each treatment, 100 GFP-positive cells were randomly selected to record the GFP–LC3 distribution inside cells as described elsewhere [Hariharan et al., 2010]. The ratio of the cells with puncta-like GFP fluorescence was shown. The data presented were from one representative experiment with triplicate repeats.

MDA DETECTION

Maleic dialdehyde (MDA) in cells was determined by the 2-thiobarbituric acid (TBA) method with reference to the kit manual.

REAL TIME RT–PCR

Total cellular RNA extraction from the cells with different treatments was carried out using Trizol reagents. After quantifying by spectrophotometry, first-strand complementary DNA (cDNA) was synthesized from 500 ng total RNA with Reverse transcription Kit following the manufacturer's instruction [Pan et al., 2010]. The sequences of primers used for PCR amplification are shown in Table I: GAPDH served as internal control to normalize the addition of cDNA among samples. MJ Opticon Monitor™ Analysis Software V.3.1.32 (Bio-Rad Laboratories, Inc.) was used to evaluate C(t) value and fold change which was considered as a measure of transcriptional alteration relating to the untreated control. Results are expressed as means ± SD (n = 3).

STATISTIC ANALYSIS

Data are expressed as the means ± SEM and statistical significance was assessed by ANOVA followed by a Turkey comparisons test using the SPSS 17 software (SPSS, Inc., Chicago, IL). A value of $P < 0.05$ was considered to be statistically significant. Data presented in this paper represent three independent experiments (n = 3).

RESULTS

THE INHIBITION OF CELL VIABILITY IN MULTIPLE CANCER CELL LINES BY D-GAL

Firstly, the cytotoxic role of high concentrations of D-gal on several malignant cell lines including two neuroblastoma cell lines (N2a and SH-SY5Y), one prostate cancer cell line (PC-3), one hepatoma cell line (HepG2), and two non-malignant cell lines (NIH3T3 and LO₂), was evaluated by MTT assay. As shown in Figure 1A, D-gal at the concentrations higher than 30 g/L inhibited the viability of all four malignant cell lines in a dose-dependent manner. On the contrary, NIH3T3 cells and LO₂ cells did not respond to D-gal (Fig. 1A). We compared the influence of D-gal and glucose on these cell lines in the parallel experiments. The results showed that up to 60 g/L of glucose did not inhibit the viability of malignant cell lines significantly (Fig. 1A), D-Gal toxicity was also supported by the observations from time course studies in which the viability of N2a cells declined to

TABLE I. Primers Used for RT-PCR Experiments

| Gene	Forward primer	Reverse primer
GAPDH	GTATGACTCCACTCACGGCAAA	GGTCTCGCTCCTGGAAGATG
Bmf	CCCTTG GGGAGCAGCCCCCTG	CAAGACAGTATCTGTCCTCCCAGAC
Bnip3	GCTCCCAGACACCACAAGAT	TGAGAGTAGCTGTGCGCTTC
Caspase-3	AACCAGATCACAAAATTCTGCAAA	TGGAGTCCAGTGAACTTTCTTCAG
Bax	CCAGGATGCGTCCACCAAG	AAGTAGAAGAGGGCAACCAC
p53	GCGTAAACGCTTCGAGATGTT	TTTTTATGGCGGGAAGTAGACTG
p21	GTGGCCTTGTCGCTGTCTT	GCGCTTGGAGTGATAGAAATCTG
Atg5	GACAAAGATGTGCTTCGAGATGTG	GTAGCTCAGATGCTCGCTCAG
TIGAR	TTCAAAATGTAACATTTTATCATCTAC	GTTTGGTTCTCTTCCTACTTCT
AR	AGG CCG TGA AAG TTG CTA TTG	ATGCTCTTGTCATGGAACGTG
Gpx3	AAACAGGAGCCTGGCGAGAACT	CCCGTTCACATCTCCTTTCTCAAA
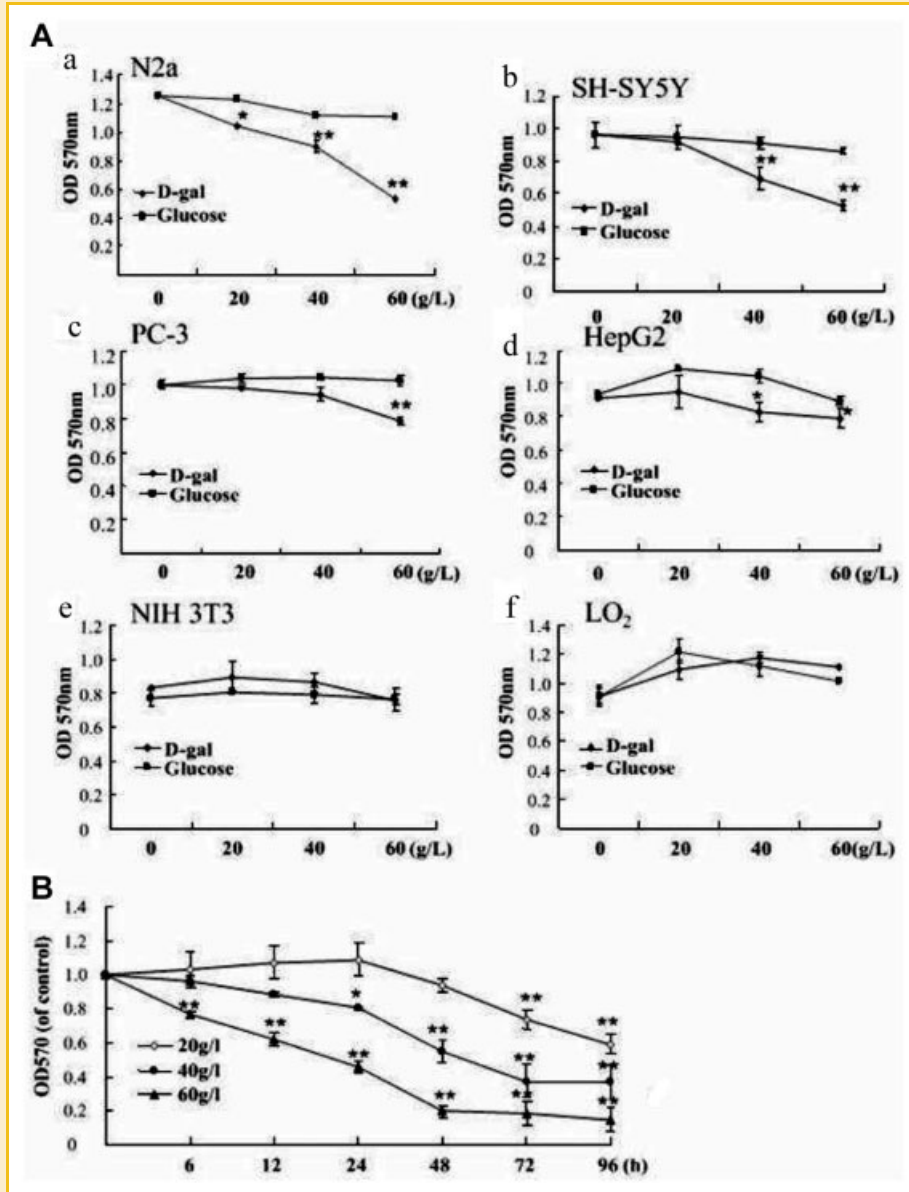
Fig. 1. D-gal decreased the cell viability of malignant cell lines. A: N2a (a), SH–SY5Y (b), PC-3 (c), HepG2 (d), NIH 3T3 (e), LO₂ (f) cells were incubated with D-gal or glucose at indicated concentrations for 24 h, (B) N2a cells were treated with 20, 40, and 60 g/L of D-gal for indicated periods. Cell viability was acquired by MTT assay. Data are representative from at least three separate experiments with each experiment quintuplicate. Data are expressed as means $\pm$ SD, n = 4. $^{*}P < 0.05$ and $^{**}P < 0.01$, compared with control, one-way analysis of variance.

about 50% after the cells were exposed to 60 g/L of D-gal for 24 h, or to 40 g/L of D-gal for 72 h (Fig. 1B). Similar results were obtained from the studies for SH-SY5Y cells (data not shown). These results display the cytotoxicity of D-gal in tested malignant cells.

ANTIPROLIFERATIVE ROLE OF D-GAL ON NEUROBLASTOMA CELLS

The influence of D-gal on the proliferation rate of neuroblastoma cells was examined. As shown in Figure 2A and B, the cell population of N2a cells was significantly decreased when above 30 g/L concentrations of D-gal were loaded, with the IC₅₀ around 60 g/L. Similar results are observed in the study for SH-SY5Y cells (data not shown). In cytometry analysis, the effect of D-gal on cell

cycle arrest was confirmed. As shown in Figure 2C, G1 was captured in N2a cells after 24 h treatment of 40 g/L D-gal and, G2/M was captured when 60 g/L D-gal was used. These results reveal the antiproliferative role of D-gal in N2a cells.

D-GAL SUPPRESSES THE COLONY FORMATION AND THE ATTACHMENT ABILITY IN N2A CELLS

Other two cell growth assays for estimating the ability of malignancy growth were performed. In colony formation assay, the number of N2a cell colony was clearly decreased after cells being treated with D-gal for 11 days (Fig. 3A,B). When the morphology of the colonies was scrutinized under higher magnifying microscope,
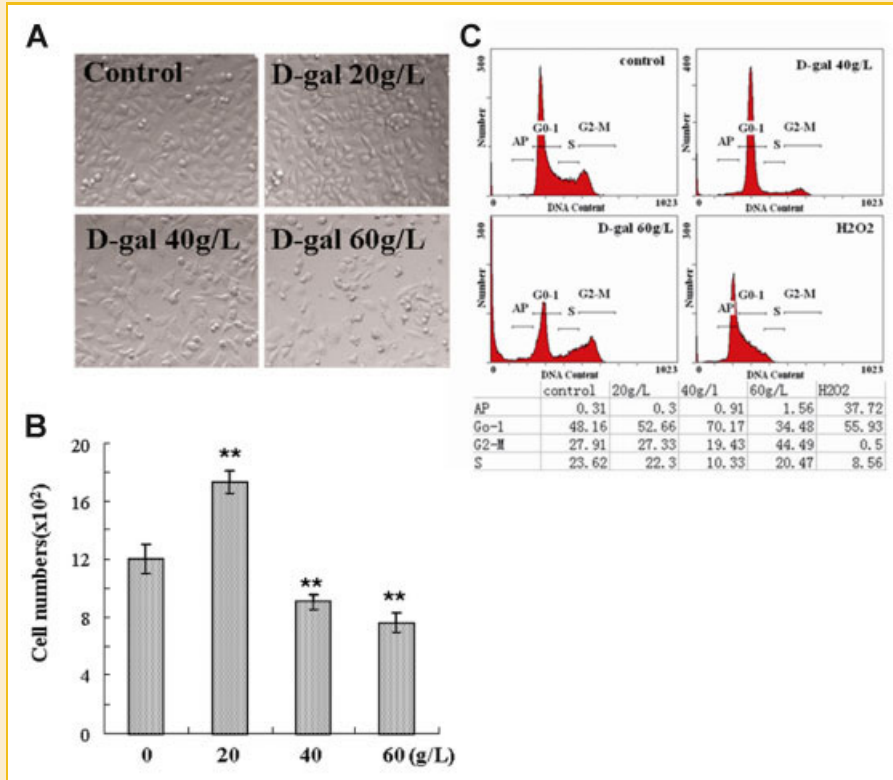
Fig. 2. D-gal induced growth inhibition in neuroblastoma cells. A: Microscopic images of N2a cells following indicated treatments, magnification, 200×. B: Cell numbers in 4 randomly selected fields were counted from the cells treated as described in (A). **$P < 0.01$ versus control group. C: Cell cycle distribution of N2a cells after incubation with D-gal for 24 h or 2 mM H_2O_2 for 2 h. The phase events from one representative experiment were shown in the table. [Color figure can be seen in the online version of this article, available at http://wileyonlinelibrary.com/journal/jcb]
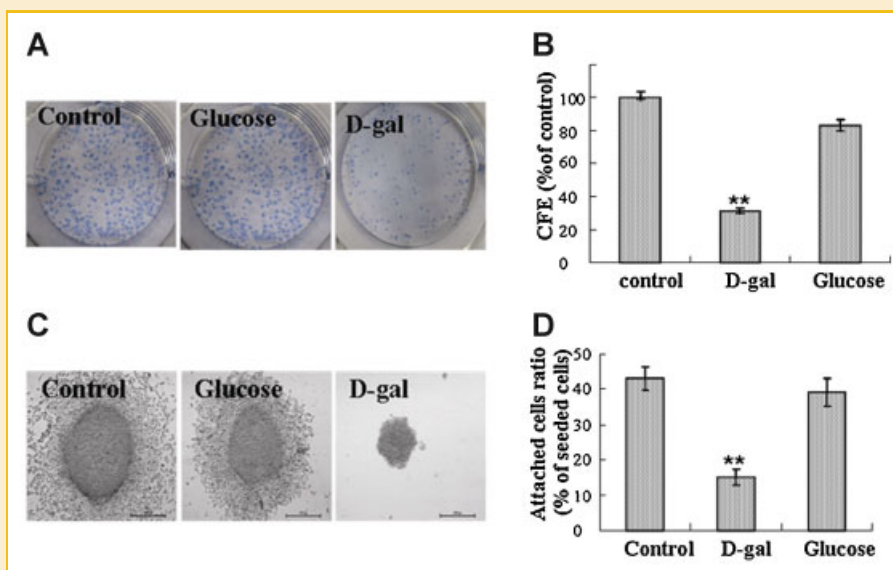

Fig. 3. D-gal attenuated the colony formation and the attachment ability of N2a cells. A: The colonies of N2a cells developed for 11 days were shown following Giemsa staining. B: Colony formation efficiency versus control group (CFE %) was presented. All data were obtained from three independent experiments, *$P < 0.05$ and **$P < 0.01$ versus control group. C: High amplified morphology of the colonies was visualized by microscopy, magnification, 400×. D: Cell attachment assay was conducted as described in the Materials and Methods Section. The percentages of attached cells against seeded cells from one representative experiment were shown. Three independent experiments were conducted. **$P < 0.01$ versus control group.

the dissimilarity was observed between the colonies growing under different conditions. The colonies in control wells were larger and surrounded by at least 10 layers of migratory cells. Differently, the cell colonies in the wells with 40 g/L of D-gal were much smaller and were surrounded by very few, if any, separating cells (Fig. 3C). Likewise, the results from cell attachment assay showed that the attachment of N2a cells on solid matrix was significantly weakened after D-gal treatment comparing to the control cells (Fig. 3D). These results demonstrate that D-gal treatment can suppress the colony formation and the abilities of matrix attachment in N2a cells.

D-GAL INDUCES CELL DEATH

Cell death was remarkably induced after high concentrations of D-gal treatment since round and floating cells were observed. To investigate D-gal-induced cell death, two pilot ways for measuring cell death were utilized: trypan blue exclusion test for necrotic death and DAPI staining for apoptotic death. Since condensed nucleolus is a typical morphologic feature of apoptosis, H_2O_2-treated cells were included as a positive model of cell apoptosis. As shown in Figure 4A, significant number of trypan blue positive cells were counted in D-gal-treated N2a cells and SH-SY5Y cells, whereas only a few cells with condensed nucleolus were present with DAPI staining after D-gal treatment (Fig. 4B, C). In addition, the results from flow cytometry analysis showed that there was no significant increase of DNA fragmentation in the cells treated by D-gal (Fig. 2C). These results show us that necrotic cell deth, instead of apoptotic death, was likely induced.

D-GAL-INDUCED DEATH OF N2A CELLS IS NOT APOPTOTIC BUT NECROPTOTIC

To further characterize the cell death induced by D-gal, two chemical inhibitors known to block unique cell death pathways were utilized. As the results, z-VAD-fmk, a pan-caspase inhibitor and an effective apoptosis blocker, did not significantly prevent the decline of cell viability induced by D-gal, but blocked the viability loss-induced by H_2O_2 (Fig. 5A). Conversely, the pre-treatment of the cells with Nec-1, a necroptotic pathway-related RIP1 kinase inhibitor, prevented D-gal-induced loss of the cell viability but did not prevent H_2O_2-induced loss (Fig. 5B). These results strengthened the notion that the necroptosis pathway may responsible for the cytotoxicity of D-gal. Next, this notion was further pursued in extended experiments. A time course assay of LDH leakage was performed as damaged cytomembrane is one of the signs of necrotic and necroptotic program cell death. The results showed that the leakage of LDH into the culture medium was observed from 6 h of D-gal treatment, being much earlier than the loss of cell viability can be detected after D-gal treatment (Figs. 1A and 5C). As cleaved Caspase 3 is one of the protein markers of apoptosis, we evaluated its levels in N2a by Western blot assay. Resultantly, there was no cleaved Caspase3 detected in D-gal treated cell lysates (Fig. 5D). Next, the expression alterations of necroptosis- and apoptosis-related genes were measured (Fig. 5E). As shown, the transcriptions of Bmf and Bnip3, maker genes of necroptosis [Hitomi et al., 2008; Kim et al., 2011], were apparently elevated after D-gal but not H_2O_2 treatment. In contrast, apoptosis-associative genes, Caspase-3, Bax
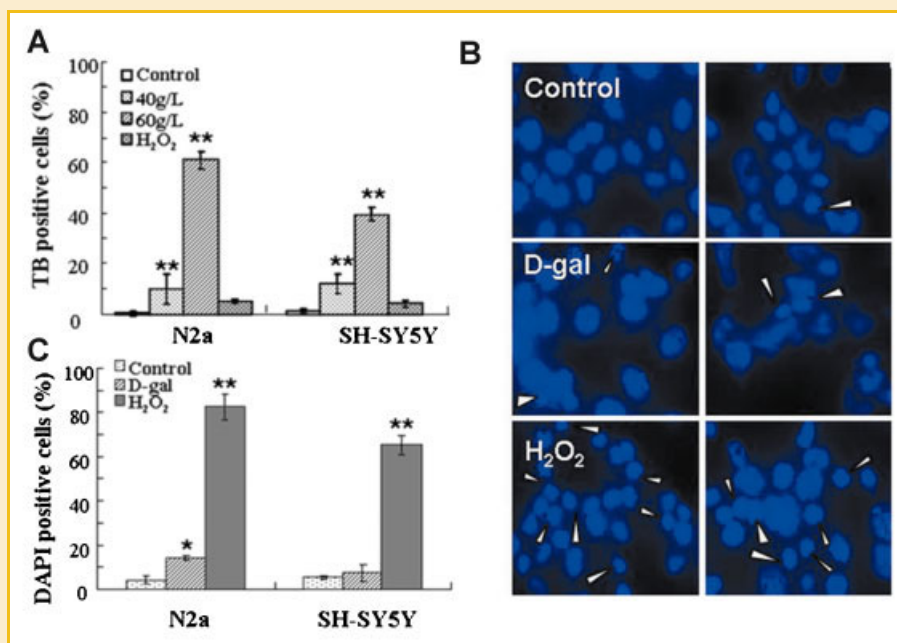

Fig. 4. D-gal induced cell death. N2a cells and SH–SY5Y cells were treated with 40 and 60 g/L of D-gal for 24 h or 2 mM of H_2O_2 for 2 h. A: Both adherent and floating cells were stained with trypan blue (TB) and counted under phase contrast microscope, the rates of TB-positive cells in total cells were shown. B: Cells were stained with DAPI and observed under fluorescence microscope. Condensed nucleoluses with DAPI staining were pointed out by white arrow head, magnification, 400×. C: The rates of condensed nucleoluses against total cells were calculated. At least 300 cells were counted. Data from one representative experiment is shown and at least three separate experiments were conducted. $^*P < 0.05$ and $^{**}P < 0.01$ versus control groups. [Color figure can be seen in the online version of this article, available at http://wileyonlinelibrary.com/journal/jcb]
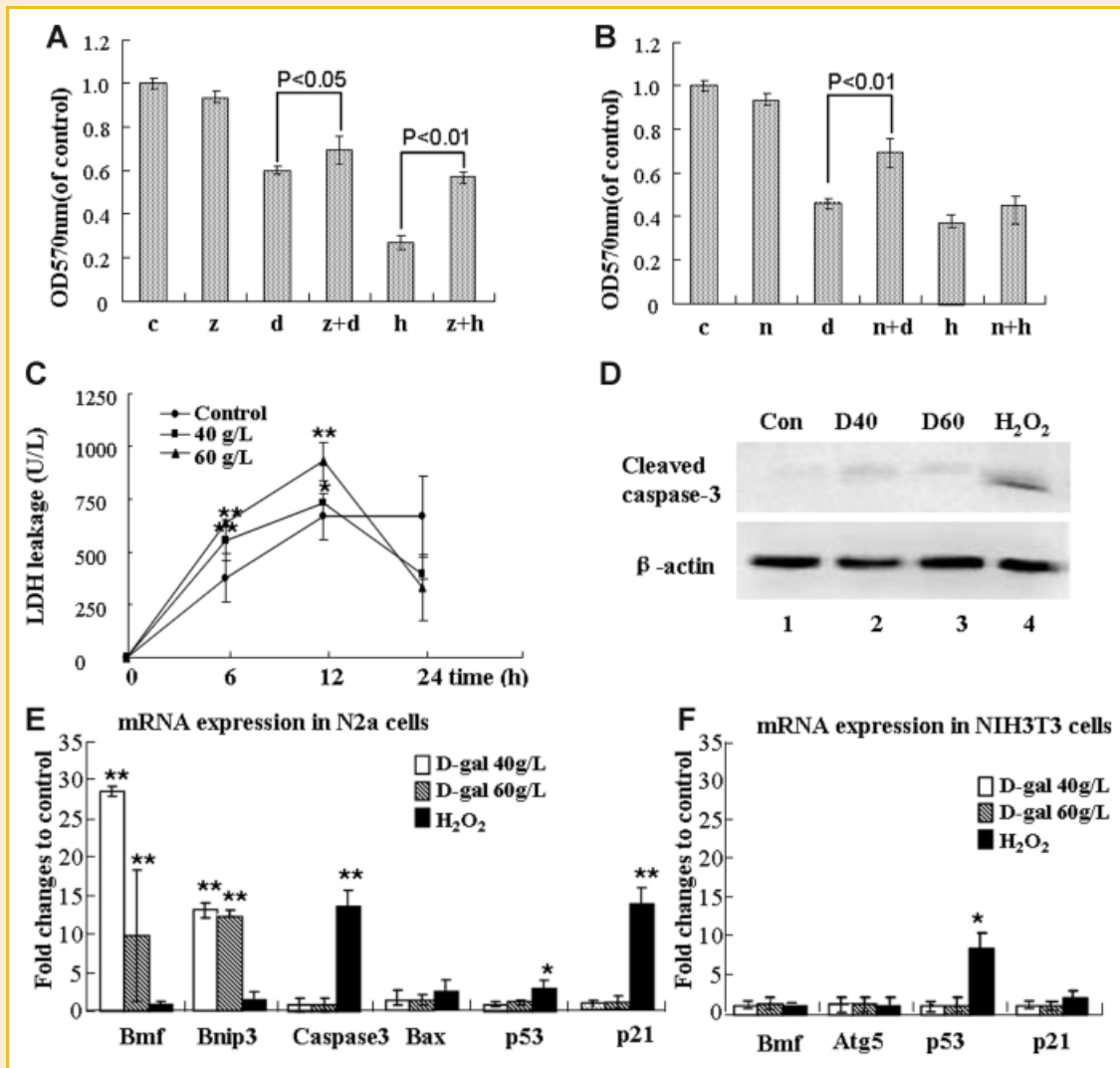
Fig. 5. The involvement of Necroptotic but not apoptotic pathway in D-gal-induced cell damage. A: Cell viability of N2a cells was evaluated in both (A and B). A: The cells accepted following treatments: untreated (c), 10 μM z-VAD-fmk (z), 60 g/L D-gal (d), D-gal plus z-VAD-fmk (z + d), 2 mM H₂O₂ (h) and H₂O₂ plus z-VAD-fmk (z + h). D-Gal treatment was consistent for 24 h and H₂O₂ treatment for 2 h, z-VAD-fmk was added 1h earlier in combinational treatments. B: The cells accepted following treatments: untreated (c), 10 μM Nec-1 (n), 60 g/L D-gal (d), or Nec-1 plus D-gal (n + d), 2 mM H₂O₂ (h) and H₂O₂ plus 1 Nec-1(n + h). D-Gal treatment was performed following 24 h after 3 h pretreatment of Nec-1, (C) LDH leakage assay was performed after the cells were incubated with D-gal at indicated concentrations for different time points. D: Western blot detection of cleaved Caspase-3 in N2a cells: untreated (Con), treated with 40 g/L D-gal (D40), 60 g/L D-gal (D60) for 24 h, and 2 mM H₂O₂ (H₂O₂) treated for 2 h. E: The mRNA levels of the genes related to necroptosis (Bmf and Bnip3), apoptosis (caspase3, Bax, p53) and p53 target gene (p21) in N2a cells were measured by real time RT-PCR assay. F: The mRNA levels of indicated genes in NIH3T3 cells. The results are shown as fold changes relative to untreated control and calculated based on the methods described in the Materials and Methods Section. Three independent experiments were performed with each assay triplicates (n = 3). *$P < 0.05$, **$P < 0.01$.

and p53, were not up-regulated after D-gal treatment, despite of their up-regulation was observed in H₂O₂-treated cells. The expression of the p21 gene was also measured due to it is a transcriptional target of p53 protein. D-Gal treatment did not significantly influence the transcription of the p21 gene, suggesting no elevated p53 function exists. In Figure 5F, we presented the results obtained from NIH3T3 cells. Different from in N2a cells, no up-regulation of necroptosis related gene Bnip3 was observed in NIH3T3 cells after D-gal treatment. The results shown in Figure 5 collaboratively support the notion that D-gal-induced cell death is essentially relevant to necroptosis rather than apoptosis.

THE INVOLVEMENT OF AUTOPHAGY IN THE TOXIC EFFECT OF D-GAL

If or not another cell death-relevant process, autophagy, is involved in D-gal-induced cytotoxicity was investigated. As shown in Fig. 6A, 3-MA, the novel inhibitor of autophagy, significantly reduced the D-gal-induced loss of cell viability. We next monitored the intracellular distribution of GFP-tagged LC3 protein, a well accepted way for detecting promoted autophagy. The results showed that upon D-gal treatment, the diffused distribution of GFP-LC3 in cytoplasm was converted to the puncta-like accumulation as visualized by fluorescence microscopy (Fig. 6B). Although the efficiency of transfecting GFP-LC3 plasmid into N2a cells was not
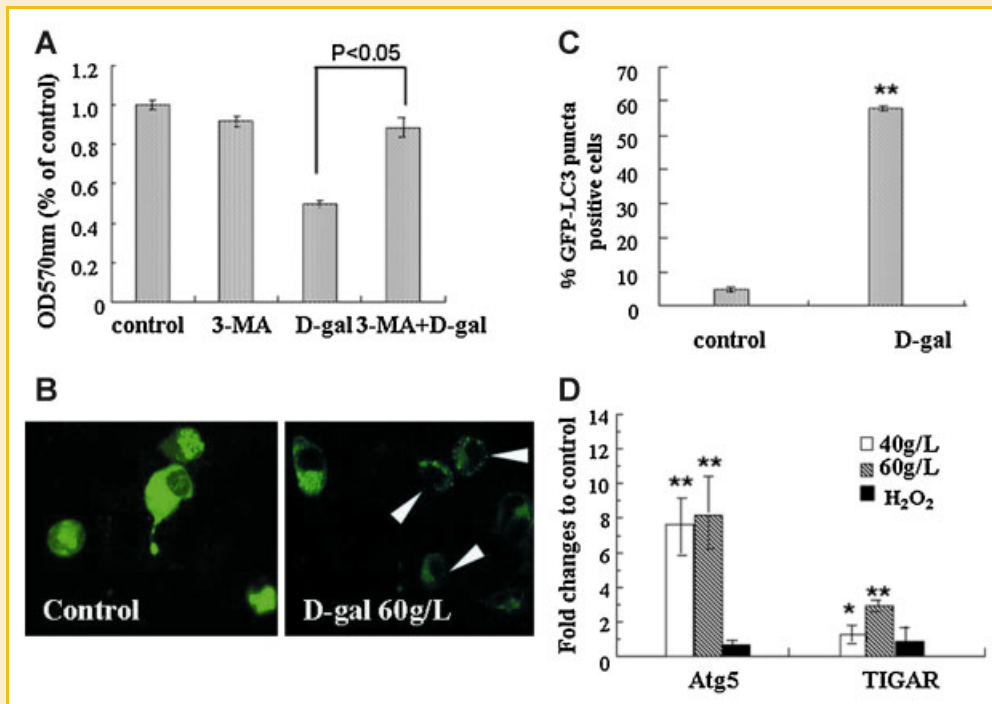
Fig. 6. The involvement of autophagy in D–gal–induced cell damage. A: N2a cells were kept untreated, or treated with 2 mM 3–MA, 60 g/L D–gal alone and 3–MA plus D–gal. Cell viability was assayed. B: N2a cells transfected with pEGFP–LC3 were untreated or exposed to 60 g/L D–gal for 24 h and observed under fluorescence microscope. Representative images were presented, magnification, 400×. C: Quantitative analysis of GFP–LC3 distribution in transfected cells as described in the Materials and Methods Section, the rate of GFP–LC3 puncta positive cells in indicated groups was assessed. D: The mRNA levels of Atg5 and TIGAR genes were measured by real time–PCR. The samples were from the cells treated by 40 and 60 g/L D–gal for 24 h, or 2 mM H_2O_2 for 2 h. Fold changes relative to untreated control were displayed. Data represent mean ± SEM; *$P < 0.05$, **$P < 0.01$. [Color figure can be seen in the online version of this article, available at http://wileyonlinelibrary.com/journal/jcb]

satisfactory, we counted 100 GFP-positive cells in total and the higher ratio of puncta-like GFP distribution was obtained from D-gal treated cells (Fig. 6C). Figure 6D shows another supportive data, in which the transcriptions of two autophagy-related genes, Atg5 and TIGAR, were up-regulated in the cells treated by D-gal. For NIH3T3 cells, however, D-gal treatment did not induce the expression of Atg5 (Fig. 5G). Above results reveal that autophagy is prompted in the D-gal treated cells and this process is relevant to the toxicity of D-gal in neuroblastoma cells.

THE INVOLVEMENT OF AR-MEDICATED POLYOL PATHWAY IN THE TOXIC EFFECT OF D-GAL

As previous studies have mentioned that AR-medicated polyol pathway is relevant to the production of oxidative stress when excessive sugar existence, we addressed the involvement of AR-mediated polyol pathway in D-gal-induced cell death. When N2a cells were pre-treated with sorbinil, a specific inhibitor of AR, the viability of D-gal-treated cells was significantly recovered (Fig. 7A). Moreover, increased mRNA levels of AR in D-gal treated cells were measured by real time RT-PCR (Fig. 7B). Considering the activation of polyol pathway usually walks along with elevated oxidative stress, anti-oxidative response and increased amounts of lipid peroxides, Gpx3 expression and MDA content were measured also. The response of Gpx3 expression on D-gal treatment was similar to that of AR expression (Fig. 7B). As shown in Figure 7C, MDA content

in D-gal treated cells increased in a dose-dependent manner. These results suggest the involvement of AR-mediated polyol pathway in the cytotoxicity of D-gal.

DISCUSSION

In this study, we demonstrate the cytotoxic effect of D-gal on several malignant cell lines, with emphasis on neuroblastoma cells. Our results reveal that D-gal can induce non-apoptotic but necroptotic cell death with potential malignancy relevance. Our results also indicate the involvements of autophagy process and AR pathway in D-gal treated cells, suggesting new underlying molecular mechanisms which trigger necroptosis. Although it is crucial to fully evaluate the antitumor effect of D-gal especially in vivo, our study has for the first time provided information on the potential antitumor effect of D-gal.

Unlike most antitumor drugs that act via suppressing cell growth and inducing apoptotic cell death, D-gal induces necroptotic cell death. Given many progressed human tumors are resistant to chemical drugs and possess mutant lesions on p53 alleles, the induction of p53-independent, non-apoptotic cell death is becoming a new line of study for cancer therapy in recent years [Hu and Xuan, 2008]. As we known, only a few compounds are evidenced as the inducer of nonapoptotic cell death in tumor cells. Hu's group
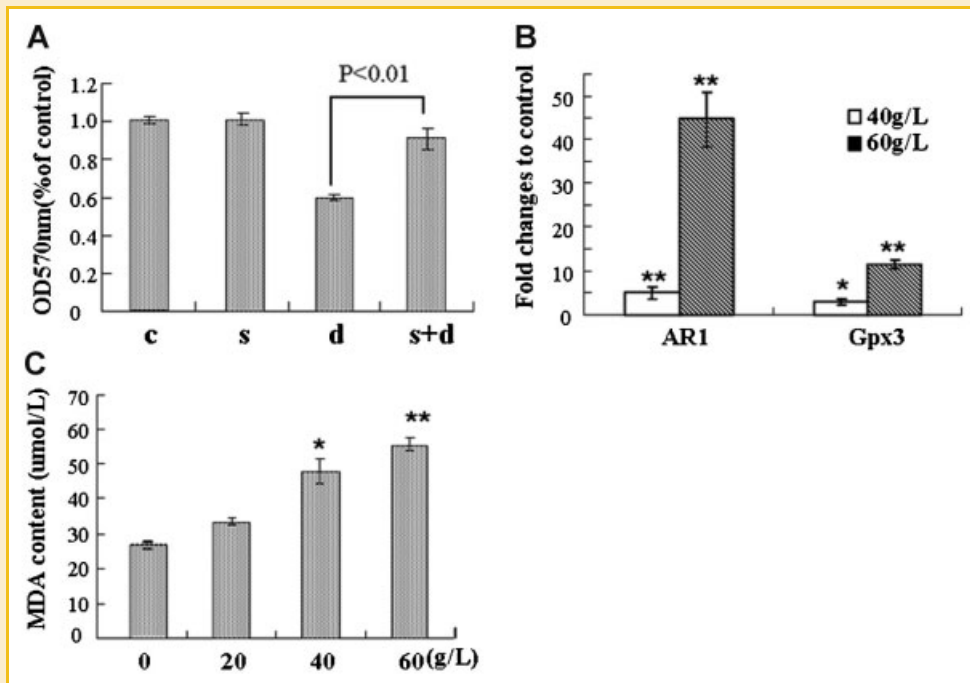
Fig. 7. The involvement of AR-mediated polyol pathway in D-gal-induced cell damage. A: N2a cells were kept untreated (c), or treated with 10 μM Sorbinil (s), 60 g/L D-gal alone (d) and Sorbinil plus D-gal (s + d) as described in the Materials and Methods section, followed by the evaluation of cell viability. B: The transcriptional expression of AR and Gpx3 genes were quantified by real-time PCR, relative fold changes were displayed. C: The MDA content in cells treated with D-gal at serial concentrations was measured. Data are expressed as means $\pm$ SD, n = 3. $^*P < 0.05$ and $^{**}P < 0.01$, compared with control, one-way analysis of variance.

reported that *shikonin* could kill drug-resistant cancer cells by inducing a dominant necroptosis [Han et al., 2007]. Xiong et al. found that autophagic cell death in Bax- or PUMA-deficient colon cancer cells following 5-FU treatment [Xiong et al., 2010]. Our results in this study reinforced the evidence that the non-apoptotic cell death can be induced in malignant cells by exogenous reagents. More importantly, the role of D-gal investigated in our study reveals for the first time that a natural hexose has the antitumor potential and probably can be used for tumor therapy, although many questions need to be answered in advance: for instance, what is the range of D-gal dosage that could be efficiently and tolerably used in vivo, and what is the suitable way of administration for a particular tumor? It is important to establish the strategy which can maximize the antitumor effect of D-gal but minimize its non-specific toxicity to normal tissues.

We evaluate the cell toxicity of D-gal is not only Caspase-independent but also p53-independent based on the facts that D-gal damaged both p53-intact malignant cell lines (N2a, SH-SY5Y, and HerpG2) and p53-mutated cancer cell line (PC-3) (Fig. 1A), and D-gal did not up-regulate the transcriptions of the p53 and p21 genes in p53-intact cells as H_2O_2 did (Fig. 5E), We consider this finding is special valuable because so many drug-resistant cancers are p53-deficient.

With regard to the higher sensitivity of malignant cells to D-gal shown in this study (Fig. 1A), it is conceivable to think about tumor specific Warburg effect, which means the increased aerobic glycolysis in cancer cells [Vazquez et al., 2010; Kim and Milner,

2011]. As aerobic glycolysis is ineffectual for ATP production, cancer cells generally uptake more sugar molecules than normal cells to fill the energy requirement [Heiden et al., 2009; Pavlides et al., 2010]. Therefore, we guess more D-gal molecules were transported into malignant cells in our system, therefore causing severer toxicity of this sugar in malignant cells than in nonmalignant cells. The experiments for testing this hypothesis are currently undertaken in our lab, by measuring of the Gluts expression and the rate of glycolysis. Nevertheless, that the prominent response of malignant cells to D-gal suggests a potential advantage of interruption of glycolysis for cancer therapy, although further studies are required for clarifying the underlying molecular mechanism.

Although previous reports have shown that some molecular connections between necroptosis and autophagy exist, the details between these two newly realized programmed cell death processes are still unknown. Thus, the finding that autophagy involved in D-gal-induced cell toxicity is certainly informative for further study. The result about the activation of AR-mediated polyol pathway is comparably interesting, because it implys us a new line of consideration: why polyol pathway could not be utilized for cancer therapy?

In this study, we focused on neuroblastoma cells because the neural specific Glut protein, Glut3, has higher affinity with D-gal than other Gluts [Arbuckle et al., 1996; Manolescu et al., 2007]. This high affinity could be beneficial for the response of neural tumors to D-gal. It should be noted that although the concentrations of D-gal

that less than 20 g/L can slightly promote the cell viability during the first day after treatment (Fig. 2B), the prolonged treatment with these concentrations had in fact delayed cell proliferation (Fig. 1B). One explanation for this phenomenon is the accumulation of galactitol, the harmful metabolite of D-gal from AR-mediated polyol pathway, needs time.

Taken together, in the present study we explored the cell toxicity of D-gal in malignant neuronal cell lines and found out that D-gal-induced cell death is non-apoptotic but necroptotic and autophagy-related. In addition, the dependency of AR-mediated polyol pathway is revealed. Our findings should be inspirational for developing anti-tumor strategies based on targeting sugar metabolism and inducing cancer cell death via non-apoptotic pathway.

ACKNOWLEDGMENTS

REFERENCES

Arbuckle MI, Kane S, Porter LM, Seatter MJ, Gould GW. 1996. Structure function analysis of liver-type (GLUT2) and brain-type (GLUT3) glucose transporters: Expression of chimeric transporters in xenopus oocytes suggests an important role for putative transmembrane helix 7 in determining substrate selectivity. Biochemistry 35:16519–16527.

Bhatnagar A, Ruef J, Liu SQ, Srivastava S, Srivastava SK. 2001. Regulation of vascular smooth muscle cell growth by aldose reductase. J Chem-Biol Interactions 130-132:627–636.

Bold RJ, Termuhlen PM, McConkey DJ. 1997. Apoptosis, cancer and cancer therapy. Surg Oncol 6:133–142.

Bonapace L, Bornhauser BC, Schmitz M, Cario G, Ziegler U, Niggli FK, Schäfer BW, Schrappe M, Stanulla M, Bourquin JP. 2010. Induction of autophagy-dependent necroptosis is required for childhood acute lymphoblastic leukemia cells to overcome glucocorticoid resistance. J Clin Invest 120(4):1310–1323.

Cho YS, Challa S, Moquin D, Genga R, Ray TD, Guildford M, Chan FK. 2009. Phosphorylation driven assembly of the RIP1-RIP3 complex regulates programmed necrosis and virus-induced inflammation. Cell 137:1112–1123.

Choi CH. 2005. ABC transporters as multidrug resistance mechanisms and the development of chemosensitizers for their reversal. J Cancer Cell Int 5:30–42.

Cui X, Li WB, Zhang BL. 1997. Establishment of the mimetic aging effect in neuron and mouse fibroblast cell by D-galactose. Chinese Appl Physiol 13:131–133. (in Chinese).

Cui X, Zuo P, Zhang Q, Li X, Hu Y, Long J. 2006. Chronic systemic D-galactose exposure induces memory loss, neurodegeneration, and oxidative damage in mice: Protective effects of R-alpha-lipoic acid. Neurosci Res 83:1584–1590.

Degterev A, Hitomi J, Germscheid M, Chen IL, Korkina O, Teng X, AbBott D, Cuny GD, Yuan C, Wagner G. 2008. Identification of RIP1 kinase as a specific cellular target of necrostatins. Nat Chem Biol 4:313–321.

Ghelli A, Zanna C, Porcelli AM, Schapira AHV, Martinuzzi A, Carelli V, Rugolo M. 2003. Leber's hereditary optic neuropathy (LHON) pathogenic mutations induce mitochondrial-dependent apoptotic death in transmitochondrial cells incubated with galactose medium. J Biol Chem 278:4145–4150.

Han WD, Li L, Qiu S, Lu Q, Pan Q, Gu Y, Luo J, Hu X. 2007. Shikonin circumvents cancer drug resistance by induction of a necroptotic death. Mol Cancer Ther 6:1641–1649.

Hariharan N, Maejima Y, Nakae J, Paik J, Depinho R, Sadoshima J. 2010. Deacetylation of FoxO by Sirt1 plays an essential role in mediating starvation-induced autophagy in cardiac myocytes. J Circ Res 107:1470–1482.

Hitomi J, Christofferson DE, Ng A, Yao JH, Degterev A, Xavier RJ, Yuan JY. 2008. Identification of a molecular signaling network that regulates a cellular necrotic cell death Pathway. Cell 135:1311–1323.

Hu X, Xuan YY. 2008. Bypassing cancer drug resistance by activating multiple death pathways—A proposal from the study of circumventing cancer drug resistance by induction of necroptosis. Cancer Lett 259:127–137.

Kabeya Y, Mizushima N, Ueno T, Yamamoto A, Kirisako T, Noda T, Kominami E, Ohsumi Y, Yoshimori T. 2000. LC3, a mammalian homology of yeast Apg8p, is localized in autophagosome membranes after processing. EMBO J 19:5720–5728.

Kim YS, Milner JA. 2011. Bioactive food components and cancer-specific metabonomic profiles. J Biomed Biotech 2011: DOI: 10.1155/2011/721213.

Kim J, Kim Y, Lee S, Park J. 2011. BNip3 is a mediator of TNF-induced necrotic cell death. Apoptosis 16:114–126.

Kowluru RA, Kern TS, Engerman RL. 1997. Abnormalities of retinal metabolism in diabetes or experimental galactosemia. IV. Antioxidant defense system. Free Radic Biol Med 22:587–592.

Krady JK, Basu A, Allen CM, Xu Y, LaNoue KF, Gardner T, Levison SW. 2005. Minocycline reduces proinflammatory cytokine expression, microglial activation, and caspase-3 activation in a rodent model of diabetic retinopathym. J Diabetes 54:1559–1565.

Kroemer G, Galluzzi L, Vandenabeele P, Abrams J, Alnemri ES, Baehrecke EH, Blagosklonny MV, EI-Deiry WS, Golstein P, Green DR, Hengartner M, Knight RA, Kumar S, Lipton SA, Malorni W, Nunez G, Peter ME, Tschopp J, Yuan JY, Piacentini M, Zhivotovsky B, Melino G. 2009. Classification of cell death: Recommendations of the nomenclature committee on cell death. Cell Death Differ 16:3–11.

Lee CH, Chou TC, Su TL, Yu JL, Shao E, Yu AL. 2009. BO-0742, a derivative of AHMA and N-mustard, has selective toxicity to drug sensitive and drug resistant leukemia cells and solid tumors. Cancer Lett 276:204–211.

Lei M, Hua XD, Xiao M, Ding J, Han QY, Hu G. 2008. Impairments of astrocytes are involved in the D-galactose-induced brain aging. Biochemand Biophy Res 369:1082–1087.

Lu J, Zheng YL, Luo L, Wu DM, Sun DX, Feng YJ. 2006. Quercetin reverses D-galactose induced neurotoxicity in mouse brain. Behav Brain Res 171:251–260.

Manolescu AR, Witkowska K, Kinnaird A, Cessford T, Cheeseman C. 2007. Facilitated hexose transporters: New perspectives on form and function. Physiology 22:234–240.

Marr HS, Edgell CS. 2003. Testican-1 inhibits attachment of Neuro-2a cells. J Matrix Biol 22:259–266.

Pan JX, Cheng C, Verstovsek S, Chen Q, Jin YL, Cao Q. 2010. The BH3-mimetic GX 15-070 induces autophagy, potentiates the cytotoxicity of carboplatin and 5-fluorouracil in esophageal carcinoma cells. Cancer Lett 293:167–174.

Pavlides S, Tsirigos A, Vera I, Flomenberg N, Frank PG, Casimiro MC, Wang CG, Pestell RG, Martinez-Outschoorn UE, Howell A, Sotgia F, Lisanti MP. 2010. Transcriptional evidence for the ''Reverse Warburg Effect'' in human breast cancer tumor stroma and metastasis: Simil arities with oxidative tress,

inflammation, Alzheimer's disease, and "Neuron-Glia Met abolic Coupling". Aging 2:185–199.

Pua HH, Zhagalov ID, Chuck M, Mizushima N, He YW. 2007. A critical role for the autophagy gene Atg5 in T cell survival and proliferation. J Exp Med 204:25–31.

Sato S, Secchi EF, Lizak MJ, Fukase S, Ohta N, Murata M, Tsai JY, Kador PF. 1996. Polyol formation and NADPH-dependent reductases in dog retinal capillary pericytes and endothelial cells. J Diabetes Complications 10:304–313.

Scheepers A, Joost HG, Schurmann A. 2004. The glucose transporter families SGLT and glut: Molecular basis of normal and aberrant function. J Parenter Enteral Nutr 28:364–375.

Tweddlea DA, Pearson ADJ, Haber M, Norris MD, Xue CY, Flemming C, Lune J. 2003. The p53 pathway and its inactivation in neuroblastoma. Cancer Lett 197:93–98.

Vander Heiden MG, Cantley LC, Thompson CB. 2009. Understanding the warburg effect: The metabolic requirements of cell proliferation. Science 324:1029–1033.

Vazquez A, Liu JX, Zhou Y, Oltvai ZN. 2010. Catabolic efficiency of aerobic glycolysis: The Warburg effect revisited. BMC Syst Biol 4:58.

Xiong HY, Guo XL, Bu XX, Zhang SS, Ma NN, Song JR, Hu F, Tao SF, Sun K, Li R, Wu MC, Wei LX. 2010. Autophagic cell death induced by 5-FU in Bax or PUMA deficient human colon cancer cell. Cancer Lett 288: 68–74.

Zhang C, Wang SZ, Zuo PP, Cui X. 2004. Protective effect of tetramethyl-pyrazine on learning and memory function in D-galactose lesioned mice. Chin Med Sci 19:180–184.

Zhong SZ, Ge QH, Qu R, Li Q, Ma SP. 2009. Paeonol attenuates neurotoxicity and ameliorates cognitive impairment induced by D-galactose in ICR mice. Neurol Sci 277:58–64.